Mathematical Biosciences and Engineering

MBE, 18(6): 9033–9049.
DOI: 10.3934/mbe.2021445
Received: 27 July 2021
Accepted: 15 October 2021
Published: 21 October 2021

http://www.aimspress.com/journal/MBE

Research article

Using a simple spectrophotometer to analyze cypress hydrolat composition

Chang-Lung Yen*, Jian-Hung Chen, Hung-Yu Chien, Jen-Son Cheng, Meng-Shiu Lee and Yueh-Ying Wang

College of Management, National Chi Nan University, Nantou County 545, Taiwan (R.O.C.)

* **Correspondence:** Email: s107245909@gmail.com; Tel: +886492910960; Fax: +886492914511.

Abstract: The Pure Dew (Cypress Hydrolat), which could be extracted from the waste material after the extracting essential oil from Taiwan cypress, has a good bactericidal effect. However, due to the high cost on quality control and concentration measurement of the Pure Dew, its application was restricted. This research tries to find suitable spectral frequencies through which the absorbance detected by the spectrometer could be used as the index of the pure dew concentration. This study used Gas Chromatography-Mass Spectrophotometer (GC-MS) to analyze the composition of Taiwan cypress hydrolat. After obtaining the composition, the raw liquor of cypress hydrolat was diluted to 100, 50, 25 and 0% v/v with pure water. The test samples were then tested by a simple spectrophotometer. After the spectrographic detection of absorbance using a simple spectrophotometer, it is confirmed that the spectrum of wavelength between 205–350 nm is the most representative. The absorptance and the pure dew concentration was roughly in linear relation which suggested that a simple spectrophotometer can be used to develop a low-cost and high.

Keywords: cypress hydrolat; GC-MS; spectrophotometer; concentration measurement

1. Introduction

Red cypress, or chamaecyparis, is only grown in a few areas around the world. Located at the southernmost region of the cypress tree distribution, Taiwan is the only subtropical area with cypress. Taiwan cypress usually refers to Meniki (Chamaecyparis formosensis) and Hinoki (Chamaecyparis obtuse), and they are the coniferous species commonly seen at intermediate high altitude in Taiwan. They have very high economic value, and are used intensively for forestation in mountains of high

attitude [1]. In the past half century, numerous researchers studied Meniki and Hinoki, exploring their habitats, physiological ecology, chemical elements, physical characteristics, and bioactivity [2].

Qualitative research was carried out for the steamed-water heat treatment on the outer bark of Hinoki (Chamaecyparis obtusa) to explore the possibility of using the residual forest biomass to produce valuable chemicals [3]. Most of Hinoki leaves contain essential oil, which is comprised of terpenoid glycoside. Raw terpenoid glycoside is extracted using traditional steamed hot water extraction on Hinoki leaves [4]. The ethanolic extracts on the bark of Hinoki can greatly inhibit fusarium and pseudomonas, and the inhibition is mainly caused by the volatile oil and non-volatile matter in the bark while neutral substances and acidic substances both have high activity towards pathogen [5]. The subject report highlighted that the cedar leaf oil of Hinoki can be used to stimulate olfactory sensation to significantly reduce the oxygenation concentration of hemoglobin in the right prefrontal cortex, as well as increase parasympathetic activities [6]. Academic studies revealed that touching Hinoki with palms is able to calm the activity on prefrontal cortex as well as increase the parasympathetic activities, and further cause physical relaxation [7]. According to the academic research, several chemical elements found on Hinoki contain terpenoids; some of them are considered good for antitumor, anti-malaria, and antimicrobial activity [8]. In terms of the application of Hinoki by dentists, the result shows that Hinoki is a strong antibacterial agent and able to carry out bactericidal action on porphyromonas gingivalis. Hinoki antibacterial agent does have a significant effect on the characteristics of the main outer membrane protein, but interferes with the antioxidant activities on bacteria [9].

Traditional extraction process of Taiwan cypress essential oil generates the by-product, hydrolat. Hydrolat is the condensate dissolved solution obtained from the distillation of logs, plants, or flowers. After the distillation during extraction process of distilling logs, plants, or flowers, it creates oil-water separation due to different density, known as hydrolat. Besides a small amount of essential oil, hydrolat contains all the water-soluble substances in logs, plants, or flowers. During the process of distillation, the oil elements that can be mixed with the odor escape to the condensation of distillation/condensation flow and are called water hydrolat along with oil-soluble oil. These hydrolats are commonly used to perfume, generic drug, food processing, aromatherapy, and traditional therapy [10]. The cypress hydrolat generated from traditional distillation is difficult to control its quality and lack of relevant hydrolat studies; thus, only essential oil is retained and the cypress hydrolat is discarded. When relevant pharmacological research and development application can be carried out, and the quality of hydrolat after distillation be controlled, there is a potential opportunity to develop high-value products.

Traditionally, Gas Chromatography-Mass Spectrometry (GC-MS) is the common approach to test the elements of hydrolat. GC-MS can identify the 35 main elements in Hinoki oil that accounts for 99.4% of the elements [11].

However, the traditional GC-MS testing methods are costly and time-consuming. The testing costs for all batches of cypress hydrolat are not economical for the industry in mass production. Hence, a rapid testing method for the quality of distilled cypress hydrolat with low cost and high efficiency is urgently needed by the industry to greatly reduce the testing time and cost, while maintaining the quality of cypress hydrolat.

In recent years, spectroscope has been wide used to collect the spectrum of an item and match it with data processing and machine learning in the fields of agriculture, food, drugs, and soil. Compared to the traditional testing technology, the spectrum of item matching with data processing and machine learning contains the advantages of non-destruction, immediacy, and low labor cost.

This study proposes a fast-testing technology on the quality of distilled cypress hydrolat based on spectrum matching, and provide the relevant experiment results.

2. Literature review

The chemical elements of Hiba, Hinoki, Sawara, and Konotegashiwa can be used on the healing tissues of wounds on human body [1]. The ethanolic extracts on the bark of Hinoki can greatly inhibit fusarium and pseudomonas, and the inhibition is mainly caused by the volatile oil and non-volatile matter in the bark while neutral substances and acidic substances are both highly active towards pathogen [2]. Touching Hinoki with palms can calm the activity on prefrontal cortex, and at the same time, increase the parasympathetic activities and further cause physical relaxation [3]. The subject report highlighted that the cedar leaf oil of Hinoki can be used to stimulate olfactory sensation to significantly reduce the oxygenation concentration of hemoglobin in the right prefrontal cortex, as well as increase parasympathetic activities [4]. Hinoki essential oil can also be used in air purifiers to repel fruit flies and house flies, and the use of 70 μg/ ml of the essential oil has an effective period of about 5 hours [5]. This study evaluated the antibacterial activity of cypress essential oil against general infectious microorganisms and clinically resistant strains. The results revealed that the essential oil and non-volatile residue contain wide inhabitance activity towards the tester strain as well as antibacterial activity towards Methicillin-resistant Staphylococcus aureus (MRSA) and Vancomycin-Resistant Enterococcus (VRE) [6].

GC-MS is a method commonly used to identify analysis for different substances in the testing samples by combining the characteristics of gas chromatography and mass spectrometry [7]. It has been widely applied in the fields of environmental and biomedicine studies, as well as bioinformatics [8]. Previous studies examined the elements in the essential oil of Hinoki leaves and its seedlings leaves, and applied factor analysis and cluster analysis using the GC-MS [9].

Headspace solid-phase microextraction (static-HS) combining with GC-MS was used to analyze 23 leave samples from three species. The results indicated the static HS process greatly enhanced the speed of precision analysis of chemical fingerprints on a small number of samples. It is a fast and reliable tool for predicting characteristics of elements in the essential oil and the analysis of essential oil elements [10]. Essential oil from the upper part of Hinoki is obtained by hydro-distillation and analyzed by GC, GC-MS and ^{1}C-NMR spectrum. The results showed that in the Hinoki oil, the main elements, such as perpinen-4 ol, SA olefin, camphor, citronellol, and γ- terpinene, account for 99.4% [11].

Hinoki residual forest biomass contains valuable chemicals, and GC-MS results also verified the content of chemical compounds [12]. Hinoki oil has great antibacterial and termite-repellent performance, without having strong bioactivity, and is a safe substance for the living environment [13]. Another study on Hinoki and terpenoids reported high performance in antibiosis, insect prevention, and antisepsis, as well as the effect of pressure relief and cancer prevention. Therefore, the terpenoids from the extracts can be used to help improving the public health through the humidifier [14].

Spectroscope captures signal on optical information and computerizes the signal to automatically display value of analysis, in order to identify the element contained in the specimens. Spectrometry time-of-flight secondary ion mass spectrometry (TOF-SIMS) is a technology with powerful functions and able to provide the chemical information on the surface of a solid sample without any chemical pre-treatment required. Compared with other technologies, the main advantage of TOF-SIMS is imaging analysis, which can directly observe the sub-micron spatial resolution of the chemical

distribution on the sample surface [15]. There are many types of spectroscope, such as infrared spectroscopy and ultraviolet spectrophotometer, which are used in the visible wavelength. A previous study compared the Raman Spectroscopy and Pyrolysis-gaschromatography and mass spectrometr (Py-GC/MS) [16]. Thermogravimetric-Fourier Transform Infrared Spectroscopy (TG-FTIR) and Py-GC/MS were used to study the pyrolysis process of bagasse and mud on the mixed samples [17]. With the advantage of low cost, the near-infrared spectroscopy used in the microelectromechanical systems can also be used to perform estimate of organic carbon and total carbon in the soil. These findings are helpful in using less expensive equipment to carry out higher-efficient future spectrum prediction on the organic carbon and total carbon in the soil [18]. In order to satisfy the demand for more complicated analysis technology, the pharmaceutical industry has used the spectrum screening technology that can be deployed at site to check the medicines that contain the elements of adulterated drugs or drugs with alternative risks [19]. Double beam spectrophotometer was used to measure site reflectance, and several sets of Analytical Spectral Devices (ASD) visible- near infrared spectroscopy were required during the process. The testing result demonstrated the necessity of relative calibration among ASD spectroscopes [20]. The data presented by ASD visible- near infrared spectroscopy has better precision. In a further study, he standard deviation of the aerial measurements was six times smaller than the hand-held measurements. Low-altitude unmanned vehicle high spectrum data was used to carry out fast and large-scale monitoring on the heavy metal content in the soil [21]. The metabolism spectrum diagram of hydrolat points out the different potential usage as the functional elements of the products in food, beverage, and cosmetic industries based on a comparison of volatile components [22]. In the biotechnology pharmaceutical industry, near infrared spectrum\ is a powerful tool for pharmaceutical forensic science. It has been used to test the discrimination between false and true artesunate antimalarial drugs [23]. Near infrared spectrum has been used to develop qualitative and quantitative methods with non-invasive modes to monitor wet granulation process. The spectrum data has been used to establish qualitative multiple modes based on the principal component analysis. The qualitative mode only uses spectrum data to monitor different procedures in granulation process [24]. Reflectance spectroscopy was used to estimate the biochemical compound concentration (tea polyphenols and total amount of free amino acid) related to the mass of tea *(Camellia sinensis (L.)*. Hyperspectral remote sensing is useful for lateral monitoring on chemical elements intea leaves [25]. As indicated in previous studies, an accurate and precise spectrum measure demonstrates the characteristics of the target material [26]. The first step of developing aflatoxin smart sorter is to confirm the critical wavelength of aflatoxin testing [27]. The reflection measurement carried out by ASD was used to predict the performance of chlorophyll on leaves [28]. The near-field optical instrument was used to obtain water quality parameter for monitoring and verifying optical satellite data [29]. According to the analysis results on the six type of hydrolats, the experimental results showed that better absorption value appears at 290~400 nm in Taiwan sandalwood hydrolat and Taiwan cypress hydrolat. Thus, they could be added to cosmetic products in the future for sun protection [30].

The monoterpenoids in the basic Chamaecyparis Obtusa oil were studied to confirm the presence of monoterpenoids in essential oils, by using gas chromatography, ultraviolet method and infrared absorption spectroscopy [31]. The spectrum of the neutral glycolipid content in the hydrolysis products revealed the existence of xylooligosaccharide, except for d-Xyl with degree of polymerization between 2 and 8. The Arabinoglucuronoxylans (AGX) from Chinese fir and H wood contains unsubstituted chain, and is consisted of at least 8 d-Xyl residues. Chemical equilibrium model and ultraviolet-visible spectrophotometer were used to estimate the copper adsorption amount on humic

acid without further instrument analysis or copper adsorption isothermal experiment [32]. A mobile laser inductive fluorescence spectrometry laser was developed to monitor the pollen floating in the air. The fluorescence spectrometry was used to measure the fluorescence spectrum of pollen released at 355 nm, and the result revealed that a peak usually appeared at 460 nm in the range of 400–600 nm [33]. Spectrum analysis and texture analysis were also adopted to extract target forest species based on color spectrophotometry [34]. However, the apparent didecyldimethylammonium chloride (DDAC) concentration on Japanese larch and western hemlock higher than the actual value was solved at 477 nm. The method also provided accurate values [35]. Scholars clarified the structure on the new compounds through spectrum methods [36].

The process does not destroy the samples and the operator can be trained rapidly and easily. Each constituent of the sample has different reflections in different spectra, these data (or spectra) can be used for identifying the constituents [37]. Amelie et al. studied fake black pepper [38], and others used honey spectrum and machine learning for rapid sieving analysis of locally representative longan and lychee honey [39].

The high-accuracy spectral radiance metering system is established according to the spectral radiance characteristic of the deuterium lamp. The consistency of spectral distribution is better than ± 5% v/v within 165~300 nm [40]. The relative spectral distributions of three spectral radiance standard neon light sources were compared and the imported error was1.7% v/v [41]. The spectrum value was about 40 and different fragrance samples showed that they can be distinguished clearly [42]. The combination of Fourier transform infrared spectral technique and multivariate analysis can analyze wood samples without time-consuming sample preparation [43]. Two methods have been developed for quantifying melamine. The correlation coefficient (R^2) values obtained by univariate analysis using CN emission spectrum band and multivariate calibration NN model are 0.982 and 0.999 respectively [44].

The spectrographic technique of the micro spectrophotometer can be quickly and easily implemented [45]. The original theoretical basis of this study is the findings of scholars. The UV absorption capacity of the hydrolat was evaluated by using a UV-vis spectrophotometer. Taiwan cypress hydrolat had better absorption at 290~400 nm. Another study used the PLSR model of 350~400 nm band for rapidly filtering low concentration cypress hydrolat samples.

3. Methods and experimental data

3.1. Research design

The experimental method can clarify the causality between variables in social science [46]. In this study, the product source of Chamaecyparis obtusa var. formosana was first confirmed, and the cypress hydrolat was distilled from the confirmed sample. The hydrolat was delivered to the notarial unit to measure the proportion of components by GC-MS. The cypress hydrolat of the same sample was diluted to 50% v/v, 25% v/v, and pure water 0% v/v.

The four samples were tested by a simple spectrophotometer and the data were acquired. The four groups of data were used for regression analysis analysis. The optimal correlation coefficient and R square wavelength interval were obtained, and then all band and optimum correlation coefficient and R square wavelength interval were used for regression statistics. The all band and optimum correlation coefficient and R square wavelength interval were compared for regression statistic of correlation.

This study used different spectral wavelengths 180~1100 nm for further discussion, in order to determine the obvious difference between wavelengths using a simple spectrophotometer. A low-cost and high-efficiency rapid sieving analysis technique was developed for managing the quality of distilled cypress hydrolat.

3.2. Material validation

The experimental was based on the "fruit of the poisonous tree doctrine", meaning that if the source is contaminated, the collected samples should also be deemed contaminated, and thus discarded [47]. As there are numerous kinds of wood, identifying cypress wood has to be based experience and wood smell is risky to some extent. If the source is not confirmed, the samples could not be used for the experiment. Thus, to confirm the wood gene, the cypress wood sample was sent to the laboratory of the Forestry Bureau, and the formal report confirmed the cypress wood (Figure 1).

Supplementary report
Taiwan Forestry Research Institute, Council of Agriculture, Executive Yuan, R. O. C. (Taiwan)
Tree and Forest Industry Report
Issue number: Forestry Research Institute ID:1092251632
Commission date: 20201203
Issue date:20201222
Verification item: Wood texture identification
Result: Chamaecyparis obtusa var. formosana
Remark: Cupressaceae

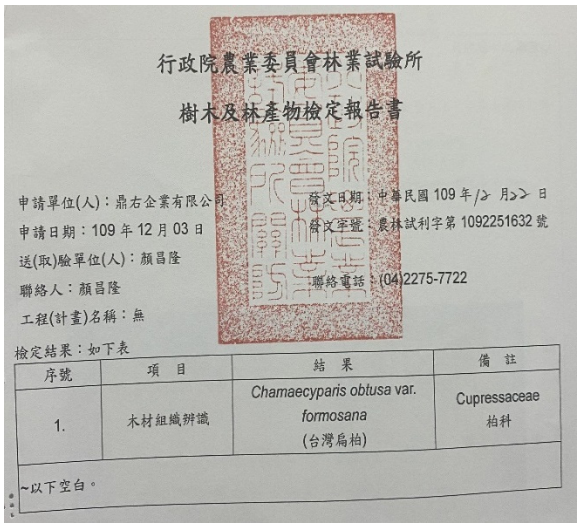
行政院農業委員會林業試驗所

樹木及林產物檢定報告書

申請單位(人)：鼎右企業有限公司　發文日期：中華民國 109 年 12 月 22 日
申請日期：109 年 12 月 03 日　發文字號：農林試利字第 1092251632 號
送(取)驗單位(人)：顏昌隆
聯絡人：顏昌隆　聯絡電話：(04)2275-7722
工程(計畫)名稱：無
檢定結果：如下表

序號	項　目	結　果	備　註
1.	木材組織辨識	*Chamaecyparis obtusa* var. *formosana* (台灣扁柏)	Cupressaceae 柏科

~以下空白。

Figure 1. FORESTRY BUREAU wood gene report.

3.3. Measuring instrument

The measuring instrument used in this study was a simple micro spectrophotometer produced by Taiwan OTO Photonics:

1) Wavelength: 180–1100 nm
2) Entrance slit: 25 um wide slit
3) Spectral Resolution: 1.2 nm FWHM
4) A/D Resolution: 16 bits
5) Integration time: 0.21 ms ~ user define
6) Fiber Optics Connector: SMA905
7) Interface: USB2.0@480Mbps (High speed)
8) Power Supply: Default USB Power
9) Dimensions: 86(W) x 110(D) x 34.6(H) mm
10) CMOS Sensor SNR: 330: 1

The instrument serial number is Model SE1030-025-FUV (Table 1)

Table 1. Serial number.

SpectraSmart Spectrum	
Spectro-Module Serial Number :	OS361AC55012029

3.4. Test material sample

After the source of cypress wood was confirmed, the cypress wood was processed to obtain hydrolat. The single sample of cypress hydrolat was sent to Forestry Bureau to test the composition by GC-MS. The cypress hydrolat composition analysis was obtained (Figures 2 and 3). As seen, α-Terpineol-35.05% v/v, Borneol-19.92% v/v, Cornphor-8.55% v/v, Fenchyl Alcohol-6.92% v/v, Terpinen-4-ol-5.59% v/v, Dihydroterpineol-4.25% v/v, Fenchone-3.06% v/v.

Supplementary report
Identification sample photos Serial number: 01Sample: Cypress Hydrolat GC-MS Test chart

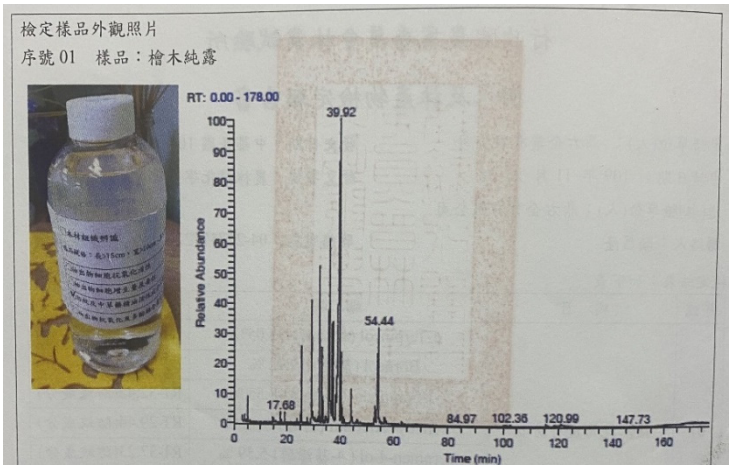

Figure 2. GC-MS test data.

Supplementary report
Taiwan Forestry Research Institute, Council of Agriculture, Executive Yuan, R. O. C. (Taiwan)
Tree and Forest Industry Report
Issue number: Forestry Research Institute
ID:1092242467 Serial number: 01
Project: Cypress Hydrolat Component analysis
Result: α-Terpineol-30.05% Borneol-19.92% (-)-Camphor-8.55% Fenchyl alcohol-6.92% Terpinen-4-ol-5.59% Dihydroterpineol-4.25% Fenchone-3.06%

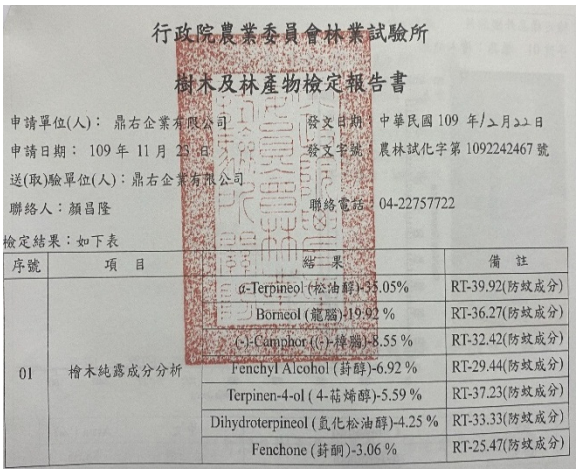

行政院農業委員會林業試驗所

樹木及林產物檢定報告書

申請單位(人)： 鼎右企業有限公司 發文日期：中華民國 109 年12月22日
申請日期： 109 年 11 月 23 日 發文字號：農林試化字第 1092242467 號
送(取)驗單位(人)：鼎右企業有限公司
聯絡人：顏昌隆 聯絡電話：04-22757722
檢定結果：如下表

序號	項 目	結 果	備 註
01	檜木純露成分分析	α-Terpineol (松油醇)-35.05%	RT-39.92(防蚊成分)
		Borneol (龍腦)-19.92 %	RT-36.27(防蚊成分)
		(-)-Camphor ((-)-樟腦)-8.55 %	RT-32.42(防蚊成分)
		Fenchyl Alcohol (葑醇)-6.92 %	RT-29.44(防蚊成分)
		Terpinen-4-ol (4-萜烯醇)-5.59 %	RT-37.23(防蚊成分)
		Dihydroterpineol (氫化松油醇)-4.25 %	RT-33.33(防蚊成分)
		Fenchone (葑酮)-3.06 %	RT-25.47(防蚊成分)

Figure 3. GC-MS test components.

3.5. Data analysis

The hydrolat was tested by spectrophotometer according to raw liquor 100, 50, 25 and 0% v/v. The absorbance data are shown in Figure 4.

The correlation coefficient represents the degree of linear correlation between two variables [48]. The determination coefficient (R^2), also known as the multiple correlation coefficient is well established in classic regression analysis [49]. Many test units still use R^2 or r as the discrimination standard of correction equation [50]. The value of the correlation coefficient R is ± 1. When R is 0, the variables are uncorrelated. When R is larger than 0, variables are positively correlated. When R is smaller than 0, the variables are negatively correlated. When R is equal to 1 or -1, the variables are correlated.

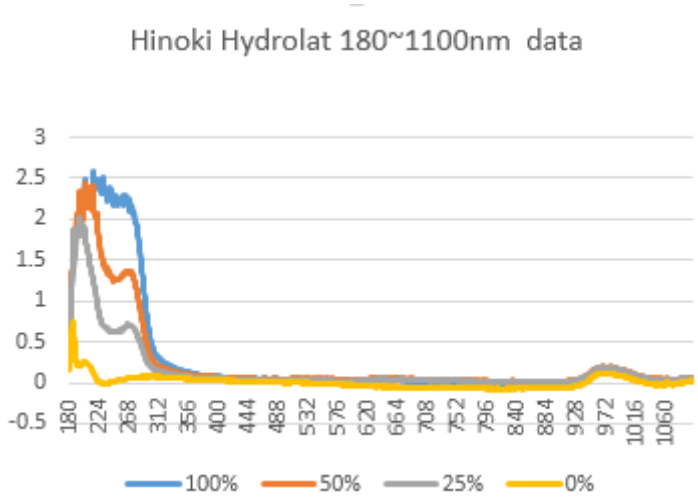

Figure 4. 180–1100 nm Hinoki Hydrolat data.

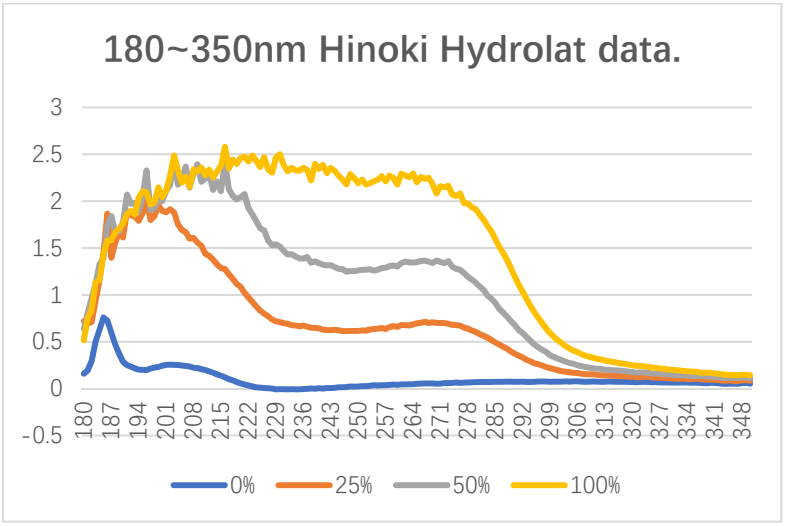

Figure 5. 180–350 nm Hinoki Hydrolat data.

In this study, the value of R square is 0~1 and the R square of the regression model is equal to 0.7, and the interpretability of this regression model for prediction result is 70%. The R square is larger than 0.75, suggesting that the model has goodness-of–fit and high interpretability.

The 100/50/25/0% v/v cypress hydrolat sample was tested by Model SE1030-025-FUV simple micro spectrophotometer. The test wavelength interval is 180–1100 nm, and the absorbance data are shown in Figures 4 and 5. As seen, the wavelength of 180–350 nm has an excellent interval difference.

The obtained cypress hydrolat samples were arranged according to 0/25/50/100% v/v, and the R square was calculated by 0% v/v basic point The computing equation is as follows.

$$R^2 = SS_{\text{Reg}} / SS_{Total} \tag{1}$$

SS_{Reg} is the amount of variation of the regression model. The SS_{Reg} computing equation is

$$SS_{\text{Re}g} = \sum \left(\hat{y}_i - \bar{y}\right)^2 \tag{2}$$

$\hat{y}_i$ is the prediction value of the regression model at point y_i. $\bar{y}$ is the average of all y_i values.

SS_{Total} is the amount of variation of y_i value and the SS_{Total} computing equation is

$$SS_{Total} = \sum \left(y_i - \bar{y}\right)^2 \tag{3}$$

The calculation results of cypress hydrolat 0/25/50/100% v/v ar.

The R correlation coefficient is 0.95, the R square value is 0.92, (Software calculation version: Microsoft Excel professional plus 2013). The regression significance value is 2.98E-78α < 0.05, the intercept P-value is 2.72E-55, the X1 variable 25% v/v P-value is 2.26E-45, the X2 variable 50% v/v P-value is 4.87E-21, the X3 variable 100% v/v P-value is 0.000671. The aforesaid dependent and independent variables are in a linear relationship. The result shows that there is a considerably fixed ratio between dependent and independent variables.

The regression equation is Y = a X + b

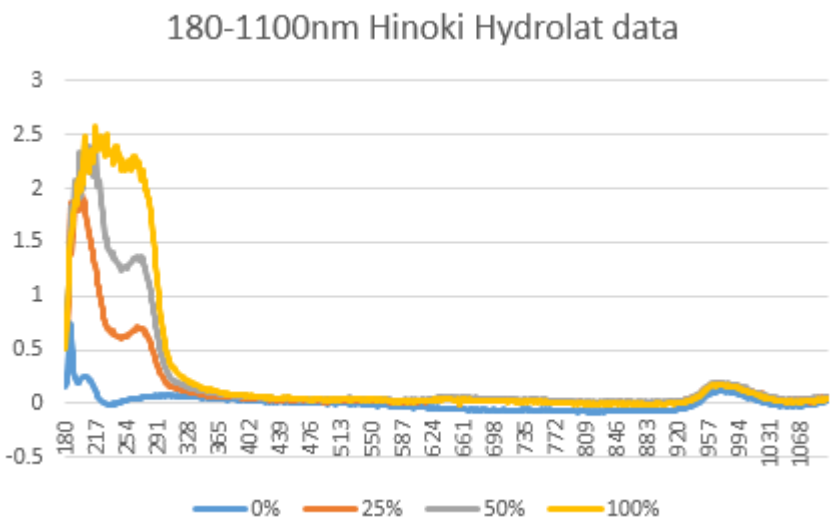

Figure 6. Hinoki Hydrolat 180~1100 nm data.

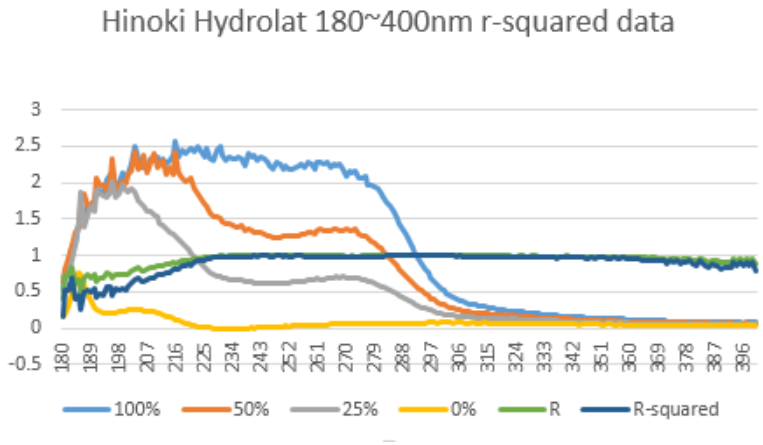

Figure 7. Hinoki Hydrolat 180~400 nm r-squared data.

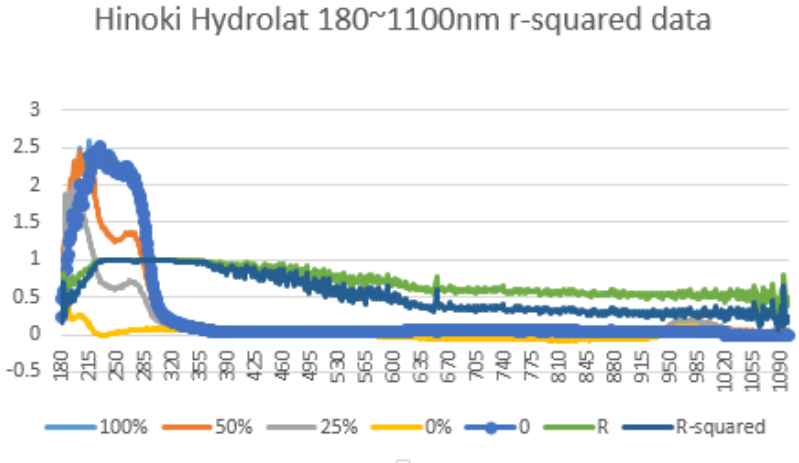

Figure 8. 180~1100 nm Hinoki Hydrolat r and R^2 data.

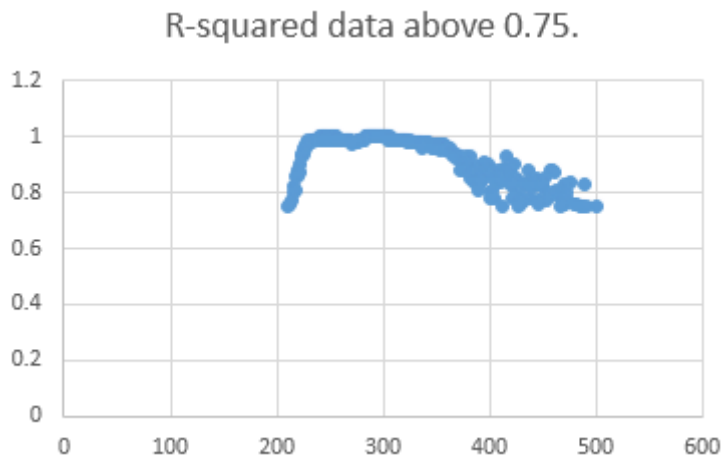

Figure 9. R-squared data above 0.75.

This study used cypress hydrolat 0% v/v as Y as a dependent variable, and 25, 50 and 100% v/v as independent variables. According to the 180–1100 nm regression statistic calculated by Excel 2013, the R correlation coefficient is 0.756864, the R square value is 0.572844, the regression significance value is 7.7E-169, the intercept P-value is 1.24E-18, the X1 variable 25% v/v P-value is 2.19E-50, the X2 variable 50% v/v P-value is 4.68E-11, the X3 variable 100% v/v P-value is 0.014315, as shown in Tables 2–4.

Table 2. 180~1100 nm regression statistics.

180~1100 nm Regression statistics	
R related	0.756864
R squared	0.572844
Adjust R	0.571446
Difference	0.054024
Number measurements	921

Table 3. 180~1100 nm ANOVA - significant data.

ANOVA	Degree of freedom	SS	MS	F	Significant data
Regression	3	3.589213	1.196404	409.9185	7.70E-169
Residuals	917	2.676393	0.002919		
sum	920	6.2656.6			

Table 4. 180~1100 nm P-value.

	Coefficient	Difference	t statistics	P-value
Intercept	-0.01779	0.001976	-9.00321	1.24E-18
X Variable 1	0.432843	0.027246	15.88665	2.19E-50
X Variable 2	-0.23439	0.035188	-6.66122	4.68E-11
X Variable 3	0.0371	0.015119	2.453937	1.43E-02

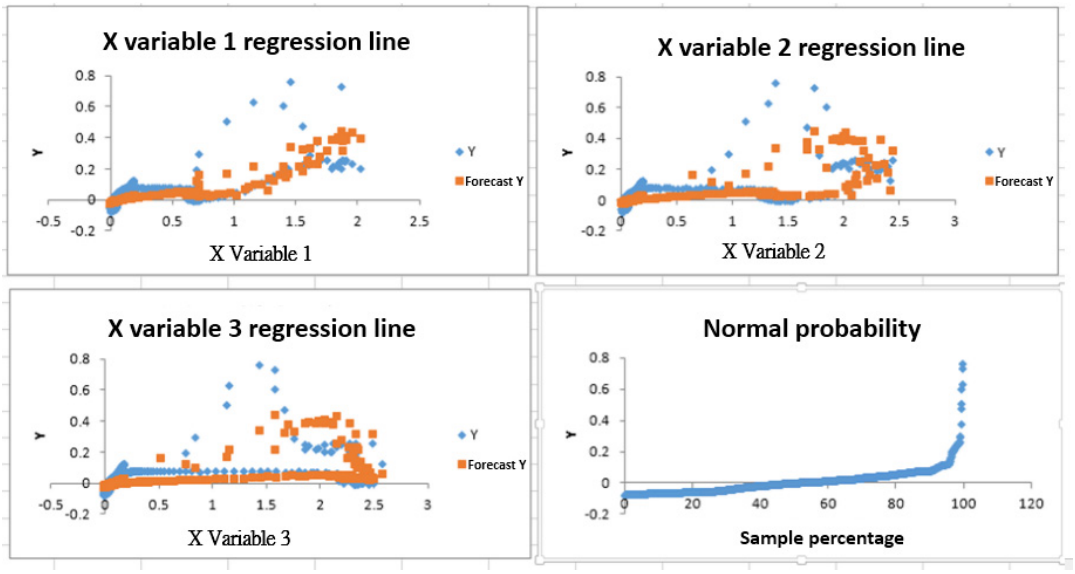

Figure 10. 180~1100 nm variable sample regression and normal probability.

The R correlation coefficient is 0.756864, the R square is below 0.75, the regression significance value is 7.7E-169α < 0.05, the intercept P-value is 1.24E-18, the X1 variable 25% v/v P-value is 2.19E-50, the X2 variable 50% v/v P-value is 4.68E-11, the X3 variable 100% v/v P-value is 0.014315. The aforesaid dependent and independent variables are not in a linear relationship, as shown in Figure 10.

This study used cypress hydrolat 0% v/v as Y dependent variable, and 25, 50 and 100% v/v as independent variables. According to the 205–350 nm regression statistic calculated by Excel 2013, the R correlation coefficient value is 0.95998, the R square value is 0.921561, the regression significance value is 2.98E-78, the intercept P-value is 2.72E-55, the X1 variable 25% v/v P-value is 2.26E-45, the X2 variable 50% v/v P-value is 4.87E-21, the X3 variable 100% v/v P-value is 0.000671, as shown in Tables 5–7.

Table 5. 205~350 nm regression statistics.

205~350 nm Regression statistics	
R related	0.95998
R squared	0.921561
Adjust R	919904
Difference	0.013797
Number measurements	146

Table 6. 205~350 nm ANOVA - significant data.

ANOVA	Degree of freedom	SS	MS	F	Significant data
Regression	3	0.317571	0.105857	556.1108	2.98E-78
Residuals	142	0.02703	0.00019		
Sum	145	0.344601			

Table 7. 205~350 nm P-value.

	Coefficient	Difference	t statistics	P-value
Intercept	0.057262	0.002227	25.71488	2.72E-55
X Variable 1	0.414892	0.019765	20.99164	2.26E-45
X Variable 2	-0.19317	0.017379	-11.1146	4.09E-18
X Variable 3	-0.01967	0.005656	-3.47794	0.000671

The R correlation coefficient is 0.95998, the R square value is 0.921561, the regression significance value is 2.98E-78α < 0.05, the intercept P-value is 2.72E-55, the X1 variable 25% v/v P-value is 2.26E-45, the X2 variable 50% v/v P-value is 4.87E-21, the X3 variable 100% v/v P-value is 0.000671. The aforesaid dependent variables and independent variables are in a linear relationship. The result shows that there is a relationship of a considerably fixed ratio between the dependent variable and independent variables, as shown in Figure 11.

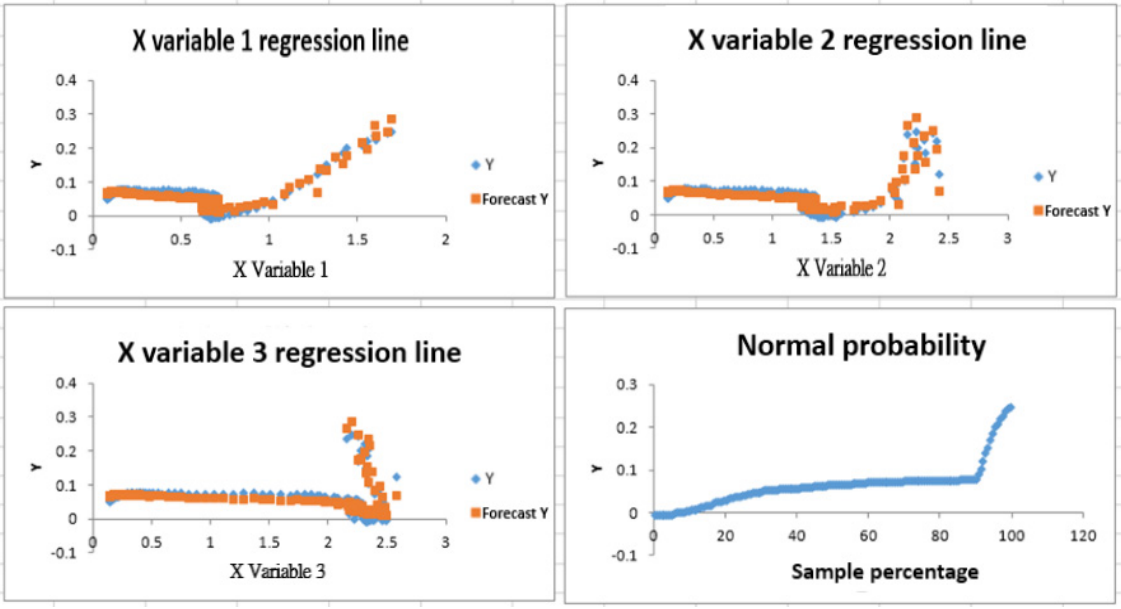

Figure 11. 205~350 nm variable sample regression and normal probability.

4. Conclusions

This study compared a simple spectrometer with GC-MS in the analysis of the composition of pure dew. To discriminate the concentrations of cypress hydrolat samples, the cypress hydrolat was diluted with pure water to liquids of 100, 50, 25% v/v, and pure water 0% v/v according to raw liquor. The samples were tested by a simple spectrophotometer. The cypress hydrolat 0% v/v is Y, a dependent variable, 25, 50 and 100% v/v are independent variables. According to 205–350 nm regression statistic calculated by Excel 2013, the R correlation coefficient value is 0.95998, the R square value is 0.921561, the regression significance value is 2.98E-78, the intercept P-value is 2.72E-55, the X1 variable 25% v/v P-value is 2.26E-45, the X2 variable 50% v/v P-value is 4.87E-21, the X3 variable 100% v/v P-value is 0.000671. The aforesaid dependent variable and independent variables are in a linear

relationship. The result shows a relationship of a considerably fixed ratio between the dependent variable and independent variables.

The experiment results of this study suggested that the absorbance of cypress hydrolat on wavelength between 205~350 nm spectrum have a linear relation to its concentration. This linear relation also suggests that a simple spectrophotometer could be sufficient to develop a low-cost, and high-efficiency rapid sieving analysis technique for managing the quality of distilled cypress hydrolat.

To obtain more accurate concentration data, some work and cost will be devoted to reproducibility tests and multi-batch tests in the future, and the quantitative prediction accuracy may be further increased.

Acknowledgments

This paper first appeared at the EIHP International Symposium in 2021 and is a revised version of the paper published at the Taiwan-Nantou County Conference in July 2021. The authors thank the organizer and Professor Yin for their guidance.

Conflict of interest

The authors declare no conflict of interest

References

1. A. Ohgaku, A. Endo, S. Hasegawa, Y. Hirose, Diterpene production by callus of some plants belonging to Cupressaceae, *Agri. Biol. Chem.*, **48** (1984), 2523–2527.
2. J. Yu, H. Komada, Hinoki (Chamaecyparis obtusa) bark, a substrate with anti-pathogen properties that suppress some root diseases of tomato, *Sci. Horti.*, **81** (1999), 13–24.
3. H. Ikei, C. Song, Y. Miyazaki, Physiological effect of olfactory stimulation by Hinoki cypress (Chamaecyparis obtusa) leaf oil, *J. Physiol. Anthropol.*, **34** (2015), 44.
4. H. Ikei, C. Song, Y. Miyazaki, Physiological effects of touching hinoki cypress (Chamaecyparis obtusa), *J. Wood Sci.*, **64** (2018), 226–236.
5. S. H. Lee, H. S. Do, K. J. Min, Effects of essential oil from Hinoki cypress, Chamaecyparis obtusa, on physiology and behavior of flies, *PLoS One*, **10** (2015), e0143450.
6. M. S. Bae, D. H. Park, C. Y. Choi, G. Y. Kim, J. C. Yoo, S. S. Cho, Essential oils and non-volatile compounds derived from Chamaecyparis obtusa: broad spectrum antimicrobial activity against infectious bacteria and MDR (multidrug resistant) strains, *Nat. Prod. Commun.*, **11** (2016), 1934578X1601100536.
7. F. G. Kitson, B. S. Larsen, C. N. McEwen, *Gas Chromatography and Mass Spectrometry: A Practical Guide*, Academic Press, 1996.
8. D. J. Beale, F. R. Pinu, K. A. Kouremenos, M. M. Poojary, V. K. Narayana, B.A. Boughton, et al., Review of recent developments in GC-MS approaches to metabolomics-based research, *Metabolomics*, **14** (2018), 152.
9. Y. Ohtani, A. Ninomiya, Z. Shibayama, K. Sameshima, Chemical distinction of hinoki [Chamaecyparis obtusa] clones made by multivariate analysis of essential oil components, *Wood Ind.*, (2002), 246–250.

10. Y. J. Chen, C. Y. Lin, S. S. Cheng, S. T. Chang, Rapid discrimination and feature extraction of three chamaecyparis species by static-HS/GC-MS, *J. Agri. Food Chem.*, **63** (2015), 810–820.
11. S. A. Emami, H. Massoomi, M. S. Moghadam, J. Asili, Identification of volatile oil components from aerial parts of Chamaecyparis lawsoniana by GC-MS and 13C-NMR methods, *J. Essent. Oil Bear. Pl.*, **12** (2009), 661–665.
12. H. Daimon, M. Faisal, Lingkungan, Preliminary investigation on the useful chemicals obtained from high-temperature and high-pressure water treatment of Hinoki (Chamaecyparis Obutus) bark, *J. Rekayasa Kimia*, **7** (2010).
13. M. J. Chung, S. S. Cheng, C. Y. Lin, S. T. Chang, Profiling of volatile compounds from five interior decoration timbers in Taiwan using TD/GC-MS/FID, *J. Wood Sci.*, **64** (2018), 823–835.
14. M. Lee, S. Park, S. Lee, H. Lee, D. Kil, Emission characteristics of volatile organic compounds by humidifier with using hinoki cypress extracts, *Mokchae Konghak J. Korean Wood Sci. Tech.*, **42** (2014), 747–757.
15. K. Saito, T. Mitsutani, T. Imai, Y. Matsushita, K. Fukushima, Application of time-of-flight secondary ion mass spectrometry to dendrochronology: estimating the felling date in discolored ancient wood by direct molecular mapping, *Anal. Chem.*, **80** (2008), 1552–1557.
16. L. Hermabessiere, C. Himber, B. Boricaud, M. Kazour, R. Amara, A. Cassone, et al., Optimization, performance, and application of a pyrolysis-GC/MS method for the identification of microplastics, *Anal. Bioanal. Chem.*, **410** (2018), 6663–6676.
17. Y. Lin, Y. Liao, Z. Yu, S. Fang, X. Ma, A study on co-pyrolysis of bagasse and sewage sludge using TG-FTIR and Py-GC/MS, *Energ. Convers. Manage.*, **151** (2017), 190–198.
18. A. Sharififar, K. Singh, E. Jones, F. I. Ginting, B. Minasny, Evaluating a low-cost portable NIR spectrometer for the prediction of soil organic and total carbon using different calibration models. *Soil Use Manage.*, **35** (2019), 607–616.
19. H. K. Srivastava, S. Wolfgang, J. D. Rodriguez, Expanding the analytical toolbox for identity testing of pharmaceutical ingredients: Spectroscopic screening of dextrose using portable Raman and near infrared spectrometers, *Anal. Chim. Acta*, **914** (2016), 91–99.
20. Y. Dung, J. Y. Lu, Q. T. Sung, Introduction of relative calibration method between ASD spectrometers, *Techn. Wind*, **14** (2016), 26–27.
21. X. S. Yi, A. J. Lan, X. M. Wen, Y. Zhang, Y. Li, Monitoring of heavy metals in farmland soils based on ASD and GaiaSky-mini, *Chin. J. Ecol.*, **37** (2018), 1781.
22. F. Ieri, L. Cecchi, E. Giannini, C. Clemente, A. Romani, GC-MS and HS-SPME-GC × GC-TOFMS determination of the volatile composition of essential oils and hydrosols (By-products) from four Eucalyptus species cultivated in Tuscany, *Molecules*, **24** (2019), 226.
23. F. E. Dowell, E. B. Maghirang, F. M. Fernandez, P. N. Newton, M. D. Green, Detecting counterfeit antimalarial tablets by near-infrared spectroscopy, *J. Pharmaceut. Biomed.*, **48** (2008), 1011–1014.
24. M. Alcalà, M. Blanco, M. Bautista, J. M. González, On-line monitoring of a granulation process by NIR spectroscopy, *J. Pharmaceut. Sci.*, **99** (2010), 336–345.
25. M. Bian, A. K. Skidmore, M. Schlerf, T. Fei, Y. Liu, T. J. Wang, Reflectance spectroscopy of biochemical components as indicators of tea (Camellia sinensis) quality, *Photogramm. Eng. Rem. S.*, **76** (2010), 1385–1392.

26. P. V. Janse, J. N. Kayte, R. V. Agrawal, R. R. Deshmukh, Standard spectral reflectance measurements for ASD FieldSpec Spectroradiometer, in *2018 Fifth International Conference on Parallel, Distributed and Grid Computing (PDGC)*, IEEE, (2018), 729–733.
27. Z. Han, L. Deng, Application driven key wavelengths mining method for aflatoxin detection using hyperspectral data, *Comput. Electron. Agri.*, **153** (2018), 248–255.
28. M. A. Cho, A. Ramoelo, A. Skidmore, Exploring various spectral regions for estimating chlorophyll from ASD leaf reflectance using prospect radiative transfer model, in *2014 IEEE Geoscience and Remote Sensing Symposium (IGARSS)*, (2014), 4754–4757.
29. A. Hommersom, S. Kratzer, M. Laanen, A. Marnix, L. Ilmar, M. Ligi, et al., Intercomparison in the field between the new WISP-3 and other radiometers (TriOS Ramses, ASD FieldSpec, and TACCS), *J. Appl. Remote Sens.*, **6** (2012), 063615.
30. L. L. Syu, S. H. Luo, J. C. Hsu, Composition analysis and antioxidant activity of six hydrolats, *Hungkuang Acad. Rev.*, **71** (2013), 77–92.
31. S. Hayashi, K. Yano, T. Matsuura, The monoterpene constituents of the essential oil of Hinoki (Chamaecyparis Obtusa (Sieb. et Zucc.) Endl.), *B. Chem. Soc. Jpn.*, **37** (1964), 680–683.
32. R. Shoji, T. Iwase, Characterization of humic acids from trees and soils analyzed by the NICA-Donnan Model and UV-Vis Spectrum, *J. Chem. Eng. Jpn.*, **50** (2017), 221–224.
33. Y. Saito, K. Ichihara, K. Morishita, K. Uchiyama, F. Kobayashi, T. Tomida, Remote detection of the fluorescence spectrum of natural pollens floating in the atmosphere using a laser-induced-fluorescence spectrum (LIFS) lidar, *Remote Sens.*, **10** (2018), 1533.
34. M. Kawamura, K. Tsujino, Y. Tsujiko, Characteristic analysis of high resolution satellite imagery for forest species discrimination, in *2004 IEEE International Geoscience and Remote Sensing Symposium (IGARSS-2004)*, **4** (2004), 2358–2361.
35. I. Momohara, A. Kato, T. Nishimura, Spectrophotometric assay of a wood preservative, didecyldimethylammonium chloride (DDAC), in aqueous solution, *J. Wood Sci.*, **56** (2010), 314–318.
36. Y. H. Kuo, C. H. Chen, S. L. Huang, New diterpenes from the heartwood of Chamaecyparis obtusa var. f ormosana, *J. Nat. Prod.*, **61** (1998), 829–831.
37. A. Rady, A. Adedeji, Assessing different processed meats for adulterants using visible-near-infrared spectroscopy, *Meat Sci.*, **136** (2018), 59–67.
38. A. S. Wilde, S. A. Haughey, P. Galvin-King, C. T. Elliott, The feasibility of applying NIR and FT–IR fingerprinting to detect adulteration in black pepper, *Food Control*, **100** (2019), 1–7.
39. H. Y. Chien, A. T. Shih, B. S. Yang, V. K. Hsiao, Fast honey classification using infrared spectrum and machine learning, *Math. Biosci. Eng.*, **16** (2019), 6874–6891.
40. Y. Liu, F. T. Li, Comparisons of two ultraviolet-vacuum ultraviolet radiation scales, *Spectrosc. Spec. Anal.*, **21** (2001), 427–431.
41. J. Xing, S. R. Wang, F. T. Li, Comparisons between radiometric scales on UV-VUV radiant standard light sources, *Opt. Precis. Eng.*, **12** (2004), 373–379.
42. K. J. Kaffka, L. S. Gyarmati, Qualitative (Comparative) analysis by near infrared spectroscopy, in *Proceedings of ICNIRS 1990*, Citeseer, (1991), 135.
43. H. Chen, C. Ferrari, M. Angiuli, J. Yao, C. Raspi, E. Bramanti, Qualitative and quantitative analysis of wood samples by Fourier transform infrared spectroscopy and multivariate analysis, *Carbohyd. Polym.*, **82** (2021), 772–778.

44. S. Moncayo, S. Manzoor, J. Rosales, J. Anzano, J. Caceres, Qualitative and quantitative analysis of milk for the detection of adulteration by Laser Induced Breakdown Spectroscopy (LIBS), *Food Chem.*, **232** (2017), 322–328.
45. D. Verma, M. Meila, A comparison of spectral clustering algorithms, *Univ. Washington Tech. Rep. UWCSE030501*, **1** (2003), 1–18.
46. C. L. Yen, Principle of experimental design and its application in sport and physical education research, *Phys. Edu. J.*, **47** (2014), 475–488.
47. W. M. Syu, Research on the application of poisonous tree fruit theory, Fo Guang University, Yilan, Taiwan, (2005), unpublished.
48. R. Taylor, Interpretation of the correlation coefficient: a basic review, *J. Diagn. Med. Sonog.*, **6** (1990), 35–39.
49. D. R. Cox, Regression models and life-tables, *J. Roy. Stat. Soc. Series B*, **34** (1972), 187–202.
50. C. C. Chen, *Comment on correlation coefficient (r) and coefficient of determination* (*R^2)*, Chung Hsing University Biological systems engineering, Available from: http://bse.nchu.edu.tw/new_page_315.htm.

AIMS Press

©2021 the Author(s), licensee AIMS Press. This is an open access article distributed under the terms of the Creative Commons Attribution License (http://creativecommons.org/licenses/by/4.0)